Journal of Chromatography A, 1437 (2016) 210–218

Contents lists available at ScienceDirect

Journal of Chromatography A

journal homepage: www.elsevier.com/locate/chroma

Development of a capillary electrophoresis method for the analysis in alkaline media as polyoxoanions of two strategic metals: Niobium and tantalum

Gauthier J-P. Deblonde[a,b,*], Alexandre Chagnes[a], Gérard Cote[a], Jérôme Vial[c], Isabelle Rivals[d], Nathalie Delaunay[c,e]

[a] Chimie ParisTech, PSL Research University, CNRS, Institut de Recherche de Chimie Paris (IRCP), F-75005 Paris, France
[b] Eramet Research, Hydrometallurgy Department, Trappes, France
[c] PSL Research University, ESPCI ParisTech, Laboratory of Analytical and Bioanalytical Sciences and Miniaturization, UMR CBI 8231, Paris, France
[d] Équipe de Statistique Appliquée, ESPCI ParisTech, PSL Research University, UMRS1158, Paris, France
[e] CNRS, UMR CBI 8231, Paris, France

ARTICLE INFO

Article history:
Received 30 November 2015
Received in revised form 26 January 2016
Accepted 27 January 2016
Available online 2 February 2016

Keywords:
Niobium
Tantalum
Capillary zone electrophoresis
Polyoxometalates
Design of experiments

ABSTRACT

Tantalum (Ta) and niobium (Nb) are two strategic metals essential to several key sectors, like the aerospace, gas and oil, nuclear and electronic industries, but their separation is really difficult due to their almost identical chemical properties. Whereas they are currently produced by hydrometallurgical processes using fluoride-based solutions, efforts are being made to develop cleaner processes by replacing the fluoride media by alkaline ones. However, methods to analyze Nb and Ta simultaneously in alkaline samples are lacking. In this work, we developed a capillary zone electrophoresis (CE) method able to separate and quantify Nb and Ta directly in alkaline media. This method takes advantage of the hexaniobate and hexatantalate ions which are naturally formed at pH > 9 and absorb in the UV domain. First, the detection conditions, the background electrolyte (BGE) pH, the nature of the BGE co-ion and the internal standard (IS) were optimized by a systematic approach. As the BGE counter-ion nature modified the speciation of both ions, sodium- and lithium-based BGE were tested. For each alkaline cation, the BGE ionic strength and separation temperature were optimized using experimental designs. Since changes in the migration order of IS, Nb and Ta were observed within the experimental domain, the resolution was not a monotonic function of ionic strength and separation temperature. This forced us to develop an original data treatment for the prediction of the optimum separation conditions. Depending on the consideration of either peak widths or peak symmetries, with or without additional robustness constraints, four optima were predicted for each tested alkaline cation. The eight predicted optima were tested experimentally and the best experimental optimum was selected considering analysis time, resolution and robustness. The best separation was obtained at 31.0 °C and in a BGE containing 10 mM LiOH and 35 mM $LiCH_3COO$.The separation voltage was finally optimized, resulting in the separation of Nb, Ta, and IS in less than 2.5 min, which is three times faster than any CE method ever reported for the separation of Nb and Ta (acidic media included). Some figures of merit of the method were determined such as linearity ranges and limits of quantitation. Finally, the method was successfully applied to the analysis of a real industrial sample.

1. Introduction

Niobium (Nb; $Z = 41$) and tantalum (Ta; $Z = 73$) are two group V elements which remain largely unknown to the general public even though they are used in several applications. Nb is primary consumed as ferroniobium (i.e. Fe–Nb alloys with at least 55 wt% Nb) in the production of high-strength low-alloy steels used in the automotive, gas pipeline and structural steel industries [1,2]. Nb

* Corresponding author at: Chimie ParisTech, PSL Research University, CNRS, Institut de Recherche de Chimie Paris (IRCP), 75005 Paris, France.
E-mail addresses: gauthier.deblonde@alumni.chimie-paristech.fr, gauthier.deblonde@gmail.com (G.J.-P. Deblonde).

http://dx.doi.org/10.1016/j.chroma.2016.01.075
0021-9673/

is also a key component of the superconducting magnets found in NMR spectrometers and in particle accelerators like the Large Hadron Collider [3,4]. Nuclear fuel claddings, optical lenses, collection coins and electronic capacitors are also among Nb-based products. With only 2 ppm in the continental crust, Ta is about ten times less abundant than Nb [5]. Hence, Ta compounds are usually more expensive than their Nb counterparts. Nonetheless, Ta is consumed worldwide for the manufacture of electronic components (capacitors, acoustic filters, touchscreen technology...) that are essential to the smartphones and other hi-tech products [6,7]. Other commercial outlets for Ta include cutting tools, high-melting point alloys, medical implants and military projectiles.

In aqueous solutions, niobium and tantalum exist only as Nb(V) and Ta(V) and are barely soluble in the usual mineral acids HCl, H_2SO_4 or HNO_3. The two ions also have the same ionic radius [8], which renders their separation very arduous both at the analytical and industrial scales [9–11]. These two strategic elements are currently produced by hydrometallurgical processes which are operated in highly acidic media and in the presence of fluoride ions (coming from NH_4F or HF) [12]. However, alkaline media (mainly NaOH or KOH-based media) are catching growing attention in the Nb–Ta industry because of the lower health risks and environmental footprint of alkaline solutions as compared to fluoride ones [13–15].

Contrasting with the increasing interest for processing Nb and Ta in alkaline media, the analytical methods for such solutions are still limited to inductively coupled plasma (ICP) spectrometry. We recently developed an UV-based method for the determination of Nb in both synthetic and industrial samples, but this method is not appropriate for tantalum [16]. A handful of capillary electrophoresis (CE) methods were also reported for the separation and quantitation of Nb and Ta, but all were performed in acidic media and the analytical times ranged between 7 and 42 min. Moreover, these methods required the addition of chromophoric and sometimes toxic reagents, like Arsenazo III, for the metal detection [17–20]. Thus, the available methods are not in line with the current approach of the Nb–Ta industry. The development of cleaner CE methods with a direct UV detection, as it has been done for other elements [21,22], would be of interest for the analytical support of the Nb–Ta industry.

We recently developed a capillary zone electrophoresis method able to separate Nb and Ta directly in alkaline media [23]. The method was only used for speciation studies and was not designed for analytical purpose. With this non-optimized method, the separation of Nb and Ta was accomplished within 6 min and the signal to noise ratio was low for both metals. This CE method took an innovative approach because it was based on the formation of $H_xNb_6O_{19}^{x-8}$ and $H_xTa_6O_{19}^{x-8}$ ions ($0 \le x \le 3$) (namely, hexaniobate and hexatantalate). These polyoxometalates are the only species that Nb and Ta form at $pH \ge 9$ and their protonation constants are 9.37 (±0.03), 10.6 (±0.5) and 13.6 (±0.2) for $H_xNb_6O_{19}^{x-8}$ and 9.3, 10.7 (±1.4) and 12.7 (±1.2) for $H_xTa_6O_{19}^{x-8}$ (at $I = 3$ M and 25 °C) [24]. They also absorb in the UV domain which allowed the direct detection of Nb and Ta ions without using chromophoric reagents. The development and optimization of a capillary zone electrophoresis method able to separate and quantify Nb and Ta directly in alkaline media could be helpful for the development of cleaner industrial processes and it is the purpose of this paper. The development of such a method was accomplished using a chemometric approach based on experimental designs [25,26]. Additional constraints, inherent to the specificity of Nb and Ta chemistries in alkaline media, also implied to use an ad hoc data treatment which allowed optimizing simultaneously multiple criteria, including analysis time, peak width and peak asymmetry.

2. Experimental

2.1. Reagents

All stock solutions were prepared with ultra-pure water delivered by a Direct-Q3 UV system (Millipore, Molsheim, France). NaCl (>99.5%), NaHCOO (>99%) and sodium naphthalene-1,5-disulfonate (98%) were purchased from Sigma–Aldrich and used without further purification. $LiOH{\cdot}H_2O$ (>98%, Alfa Aesar), LiCl (>99%, Fluka), $LiCH_3COO{\cdot}2H_2O$ (reagent grade, Alfa Aesar), and $NaCH_3COO$ (>99.0%, VWR AnalaR NormaPur®) were used as received. NaOH solutions were prepared from standardized solutions (Prolabo Normadose). $Na_7HNb_6O_{19}{\cdot}15H_2O$ and $Na_8Ta_6O_{19}{\cdot}24.5H_2O$ were synthesized and characterized as previously reported [16,27]. Stock solutions of Nb(V) and Ta(V) were prepared by dissolution of $Na_7HNb_6O_{19}{\cdot}15H_2O$ and $Na_8Ta_6O_{19}{\cdot}24.5H_2O$ in deionized water, respectively, and filtered at 0.20 μm with a syringe filter (Minisart® RC25, Sartorius) before CE experiments.

An alkaline industrial solution of Nb and Ta, coming from a hydrometallurgical process, was provided by Eramet Research (Trappes, France). The pH of the sample was 12.4. The ICP-AES analysis provided by Eramet Research is as follows: $[Nb_6O_{19}] = 3.40$ (±0.17) mM; $[Nb_5TaO_{19}] = 0.227$ (±0.011) mM. Impurities in the sample were: [Na] = 54 (±3) mM; [S] = 1.09 (±0.05) mM; [Ti] = 0.104 (±0.005) mM and [Fe] = 0.023 (±0.002) mM.

2.2. Electrophoretic conditions

All CE experiments were carried out with an Agilent Technologies 7100CE system (Massy, France) equipped with a diode array detector (deuterium lamp). The detection wavelength, detection bandwidth, reference wavelength and reference bandwidth for Nb and Ta were optimized, as discussed below. Separations were performed in a 30 cm (effective length: 8.5 cm) × 50 μm ID fused-silica capillary (Photonlines, Marly-le-Roi, France). A personal computer using HP 3D ChemStation controlled the HP 7100CE instrument and allowed data analysis. New capillaries were activated by flushes under approximately 1 bar with 1 M NaOH (or 1 M LiOH), then 0.1 M NaOH (or 0.1 M LiOH) and water (10 min each). Every day, the capillary was flushed under 1 bar for 10 min with 0.1 M NaOH (or 0.1 M LiOH) followed by the desired background electrolyte (BGE) for 10 min. All stock solutions were filtered using 0.20 μm syringe filters (Ministart®, Sartorius) before preparing the samples used for CE analysis. The BGEs were prepared less than 24 h before their injection in the CE system. The BGEs were composed of 10 mM of NaOH in addition to NaCl, NaHCOO or $NaCH_3COO$ with a total ionic strength limited to 100 mM. The corresponding Li^+-based BGEs were also studied. Nb and Ta stock solutions were stored at 4 °C and renewed every week. The samples were hydrodynamically injected at the anodic end at a pressure of 10 mbar for 3 s (about 0.3% percent of the capillary volume at 25 °C). Afterwards, the desired voltage was applied at the injection end. The CE cartridge was thermostated. Before each experiment, the capillary was flushed with the BGE for 10 min. At the end of the day, the capillary was flushed with Ultra-Pure water for 15 min. pH measurements were performed with a 827 pH-lab (Metrohm) pH-meter and low alkaline error combined electrode (Unitrode, Metrohm). The pH-meter was calibrated with NIST standards at pH 4.00, 7.00 and 10.00.

2.3. Experimental design

2.3.1. Choice of the factors, variation domains and responses

The three most important parameters that are likely to affect the separation of $H_xNb_6O_{19}^{x-8}$ and $H_xTa_6O_{19}^{x-8}$ ions are the temperature, the ionic strength and the nature of the alkaline

Table 1
Central composite design.

Block	Experimental order	Factor 1: ionic strength[a]	Factor 2: temperature[b]
I	1	0	0
	2	−1	+1
	3	−1	−1
	4	+1	−1
	5	+1	+1
	6	0	0
II	7	0	0
	8	+1	0
	9	−1	0
	10	0	0
	11	0	+1
	12	0	−1
	13	0	0

[a] Coded values: −1 = 25 mM; 0 = 50 mM; +1 = 75 mM.
[b] Coded values: −1 = 25 °C; 0 = 32.5 °C; +1 = 40 °C.

counter-ion of the BGE (the latter influences the solution chemistry of $H_xNb_6O_{19}{}^{x-8}{}_{(aq)}$ and $H_xTa_6O_{19}{}^{x-8}{}_{(aq)}$ [27–29]). Temperature and ionic strength are continuous factors whereas counter-ion nature is not. Consequently, T and I were selected as the two factors used for a design of experiments, which would be carried out for each tested counter-ion. The selected domains were: $25 \le I \le 75$ mM and $25 \le T \le 40$ °C. The tested counter-ions were Na^+ and Li^+. For quantitation purpose, an internal standard (IS) was added to the samples and, as a consequence, the separation of the three peaks (corresponding to Nb, Ta and IS) was required. The choice of IS is detailed in Section 3.1. The responses measured to evaluate the quality of the separation were the peak start, peak migration and peak end times of Nb, Ta and IS.

2.3.2. Central composite design and models

The experimental designs consisted of a central composite design with three levels for each factor (ionic strength and temperature). The center point was also repeated 5 times to evaluate the experimental error. Each experimental design corresponds to 13 experimental conditions (Table 1). Because of peak overlapping in the case of LiOH–$LiCH_3COO$ BGE, Nb and Ta were injected separately for some points. The experimental results corresponding to the two counter-ions are given in Table S1.

The relationship between the factors and a response Y (peak start, migration or end time or Ta, Nb or IS) was modeled by a full second-degree polynomial law:

$$Y = \theta_0 + \sum_{i=1}^{2} \theta_i x_i + \sum_{i=1}^{2} \theta_{ii} {x_i}^2 + \theta_{12} x_1 x_2 + W$$

where x_1 and x_2 denote the factors to be optimized (ionic strength and temperature, respectively), θ_0, θ_i, θ_{ii}, and θ_{12} the constant, affine, quadratic and first-order interaction parameters, respectively, and W the experimental error. The model parameters were estimated using ordinary least squares multiple regressions. Thanks to the repetitions at the center, the models could be tested for lack of fit [30]: for both counter-ions, all the models could be considered as unbiased ($p \gg 5\%$).

Using the Na counter-ion, the coefficients of variations of the peak times were of the order of 15%. All the linear effects were significant with a type I error risk of 5%, but the nonlinear effects were not, be the tests performed with the residual or the pure error mean squares for variance estimation. Using the Li counter-ion, the coefficients of variations of the peak times were of the order of 3% and all the effects were significant at the 5% level except for the temperature quadratic term.

2.3.3. Optimization of the separation

The goal was to find an optimal separation conditions in terms of analysis time and resolution between peaks. However, due to changes in the migration order of Ta, Nb and IS (see Table S1), neither analysis time nor resolution were continuous functions of the factors to be optimized. Thus, we developed a strategy based on the systematic evaluation of the constraints to be satisfied and of the criteria to be optimized in the whole experimental domain using the predictions of the previously validated models. The 2D experimental domain was divided in elementary pixels of width 0.1 (hence a total of $21 \times 21 = 441$ pixels) and, for each of them, the time intervals between the three possible pairs of peaks were estimated using the models of normalized peak start and peak end times:

$$\Delta t_{ij}(k) = \max_{i,j} \left(t_i^{start}(k) - t_j^{end}(k), t_i^{start}(k) - t_j^{end}(k) \right)$$

where i and j index the peaks ($i, j = 1$–3, $i < j$, i.e. 3 different couples) and k indexes the elementary pixel ($k = 1$–441). In addition, the predicted peak times were used to compute the peak widths (i.e. the $w_i(k) = t_i^{end}(k) - t_i^{start}(k)$ as well as the peak asymmetry coefficients $a_i(k)$ defined as:

$$a_i(k) = \frac{\left| \left(t_i^{end}(k) - t_i^{mig}(k) \right) - \left(t_i^{mig}(k) - t_i^{start}(k) \right) \right|}{t_i^{end}(k) - t_i^{start}(k)}$$

The analysis time, i.e. the peak end time of the last migrating component, which is not always the same one, was also predicted for each pixel as $T(k) = \max_i \left(t_i^{end}(k) \right)$. For each pixel k, we chose to:

1) impose model consistency, i.e. $t_i^{start}(k) < t_i^{mig}(k) < t_i^{end}(k)$ (hard constraint which proved to be satisfied everywhere for both counter-ions)
2) impose strictly no peak overlap, i.e. $\Delta t_{ij}(k) > \Delta t_{\min} = 0.1$ min (hard constraint),
3) optimize the resolution by either minimizing the peak widths $w_i(k)$, or maximizing their asymmetry coefficient $a_i(k)$,
4) minimize the analysis time $T(k)$,
5) as an option, optimize robustness by maximizing the number of neighboring pixels satisfying the hard constraints (1) and (2) $n(k)$ (a value between 0 and 8 for pixels inside the experimental domain, but between 0 and only 3 for a factorial pixel).

In order to perform the simultaneous optimization of (3), (4) and (5), we chose a desirability approach. The desirability function [31] was defined in each pixel as a function of the analysis time, of the peak widths (D_w) or of their asymmetry coefficients (D_a), and of their numbers of neighboring satisfying the hard constraints, i.e.:

$$\begin{cases} D_w(k) = d(T(k), T_0, T_1) \times \prod_{i=1}^{3} d(w(k), w_0, w_1) \times d(n(k), w_0, w_1) \\ D_a(k) = d(T(k), T_0, T_1) \times \prod_{i=1}^{3} d(a(k), w_0, w_1) \times d(n(k), w_0, w_1) \end{cases}$$

where $d(t, x_0, x_1)$ is Derringer type function [32], i.e. a continuous piece-wise linear function with values in [0; 1] and:

$$d(t, x_0, x_1) = \frac{t - x_0}{x_1 - x_0} \text{ if } t \in [\min(x_0, x_1); \max(x_0, x_1)]$$

and whose value is equal to 0 or 1 outside this interval in a continuous fashion. Based on the distributions of the analysis time, peak

width and symmetry coefficient, the following parameter values where chosen:

- analysis time: $T_0 = 6, T_1 = 4$, in minutes;
- peak width: $w_0 = 0.4, w_1 = 0.2$, in minutes;
- asymmetry: $a_0 = 0.3, a_1 = 0$.

For the number of neighbors satisfying the hard constraints, we chose either $n_0 = 4$, $n_1 = 8$, or $n_0 < n_1 < 0$ (robustness constraint relaxed).

Thus, depending on whether peak widths or asymmetries were minimized, and whether the robustness constraint on the neighbors was relaxed or not, we obtained 4 predicted optima for each counter-ion, see Table 2.

3. Results and discussion

3.1. Preliminary tests: detection conditions, BGE co-ion and internal standard

In a previous study [23], we showed that hexaniobate and hexatantalate ions could be separated using a classical bare-fused silica capillary having a total length of 35 cm and an effective length of 8.5 cm. The non-optimized method allowed separating Nb and Ta anions in about 6 min with a resolution superior to 5. This short effective length was thus kept and the injected sample volume was adapted to prevent from band-broadening.

In the non-optimized CE method that we previously reported for the Nb–Ta separation in alkaline media [23], the detection was done at 240 (±2) nm for Nb and 214 (±2) nm for Ta, and the reference wavelength was set at 340 (±40) nm. We here performed a systematic study in order to find the best detection conditions for Nb and Ta. The results given in Fig. S1 show that the highest signal to noise ratio is obtained when $\lambda_{det} = 211$ (±4) nm and $\lambda_{ref} = 325$ (±20) nm for Nb and $\lambda_{det} = 211$ (±5) nm and λ_{ref} 325 (±50) nm for Ta. For Nb, the detection at 211 (±5) nm with a reference at 325 (±50) nm also gives a high signal to noise ratio. Thus these parameters were selected so that both metals could be detected at the same wavelength, which facilitates the data treatment of the experimental designs. These parameters improved the signal to noise ratio by a factor of 2.3 for Nb and 6.1 for Ta.

Previously reported results [23] showed that the ratio between the effective electrophoretic mobility of $H_xNb_6O_{19}^{x-8}$ and that of $H_xTa_6O_{19}^{x-8}$ increases slightly between pH 9 and 13 and that this ratio is higher in Li^+-based and Na^+-based BGE as compared to K^+-based BGE. Therefore, the K^+-containing media were not studied in the present work. In order to keep a sufficient buffer capacity and to be able to vary the ionic strength of the BGE while keeping it lower than 100 mM (to avoid uncontrolled heating by Joule effect), we decided to perform the Nb–Ta separation at pH 12. This means that the BGE were composed of 10 mM LiOH or 10 mM NaOH in addition to a Li^+-based or a Na^+-based salt. Since the $H_xNb_6O_{19}^{x-8}$ and $H_xTa_6O_{19}^{x-8}$ ions absorb in the low-UV range, the nitrate, thiocyanate and carbonate ions are not suitable co-ions. Among the usual co-ions used in CE, Cl^-, $HCOO^-$ and CH_3COO^- were tested (Fig. 1).

As shown in Fig. 1, the symmetry for both Nb and Ta peaks is better in the presence of acetate co-ions. These results are in accordance with the measured effective electrophoretic mobilities of $H_xNb_6O_{19}^{x-8}$ (-61×10^{-5} cm^2 s^{-1} V^{-1}) and $H_xTa_6O_{19}^{x-8}$ (-54×10^{-5} cm^2 s^{-1} V^{-1}) ($I = 15$ mM and $T = 25$ °C) [18], which are closer to the absolute electrophoretic mobility at infinite dilution at 25 °C of CH_3COO^- (-57×10^{-5} cm^2 s^{-1} V^{-1}) than those of Cl^- (-79×10^{-5} cm^2 s^{-1} V^{-1}) and $HCOO^-$ (-42×10^{-5} cm^2 s^{-1} V^{-1})

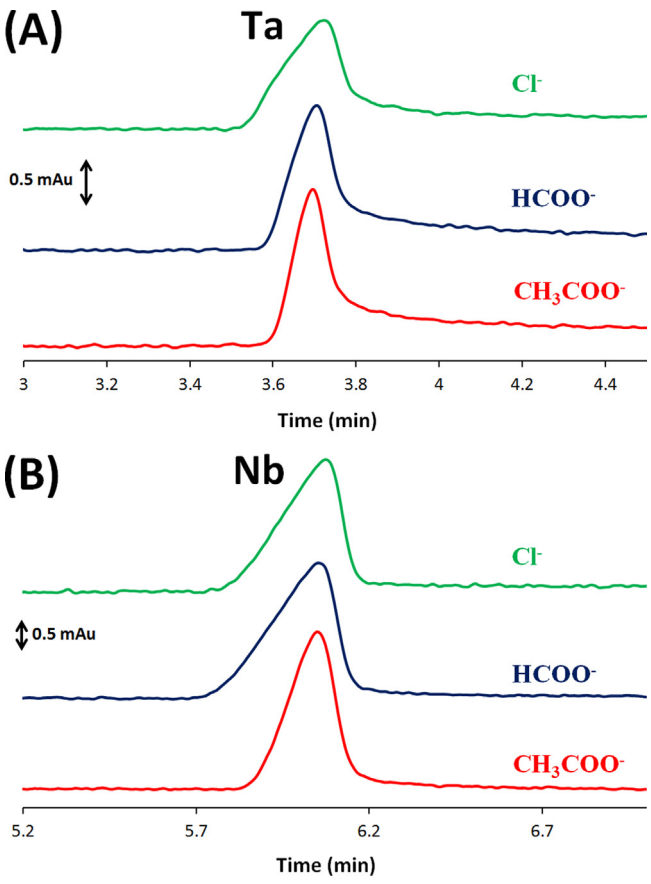

Fig. 1. Peak shapes for $H_xTa_6O_{19}^{x-8}$ ions (A) and $H_xNb_6O_{19}^{x-8}$ (B) obtained by CE in 10 mM NaOH + 40 mM NaCl (green curve), 10 mM NaOH + 40 mM NaHCOO (blue curve) and 10 mM NaOH + 40 mM $NaCH_3COO$ (red curve). $[Ta_6O_{19}] = 0.10$ mM, $[Nb_6O_{19}] = 0.10$ mM. $T = 25.0$ °C. CE conditions: bare-fused silica capillary, 50 μm ID × 30 cm (detection at 8.5 cm). Hydrodynamic injection at the anodic end: 3 s, 10 mbar. Applied voltage: 10 kV at the injection end. Detection: direct UV, $\lambda_{det} = 211$ (±5) nm and $\lambda_{ref} = 325$ (±50) nm.(For interpretation of the references to color in this figure legend, the reader is referred to the web version of this article.)

[33]. Hence, all CE experiments were carried out in LiOH–$LiCH_3COO$ or NaOH–$NaCH_3COO$ based BGEs.

In order to perform a quantitative determination of Nb and Ta, an internal standard (IS) had to be found. The internal standard should not interact with $H_xNb_6O_{19}^{x-8}$ and $H_xTa_6O_{19}^{x-8}$ ions, be stable at pH 12, should absorb the UV light and must have an electrophoretic mobility close but different to the ones of $H_xNb_6O_{19}^{x-8}$ and $H_xTa_6O_{19}^{x-8}$ ions. Based on the literature data, the naphthalene sulfonic acid derivatives were expected to fulfill these requirements. Among the tested candidates, naphthalene-1,5-disulfonate ion was found to be a suitable internal standard. The two pK_a values for naphthalene-1,5-disulfonate are lower than 1 [34], so that it is completely deprotonated under our CE conditions (pH 12).

3.2. Prediction of the optimum separation conditions

As expected, preliminary tests confirmed that the two most important parameters that affect the separation of $H_xNb_6O_{19}^{x-8}$ and $H_xTa_6O_{19}^{x-8}$ ions are the temperature (T) and the ionic strength (I). A design of experiments involving these two factors was selected. The investigated domain for ionic strength was chosen considering a short analysis time for its inferior value and the solubilities of $H_xNb_6O_{19}^{x-8}$ and $H_xTa_6O_{19}^{x-8}$ in the BGEs and Joule heating for its superior value. For temperature, the minimum value was set at 25 °C to keep a short analysis time and due to solubility considerations and the maximum value was fixed at 40 °C. Even

Table 2
Predicted optima for each counter-ion. It is chosen either to minimize peak width or asymmetry, either with or without the robustness constraint on the number of neighbors. x_1 = ionic strength, x_2 = temperature, given in coded values. The detailed analysis of the optimum of cell highlighted in grey is given in Fig. 3.

	Na^+		Li^+	
	Robustness−	Robustness+	Robustness−	Robustness+
Peak width	$x_1 = -0.4, x_2 = 1$	$x_1 = -0.3, x_2 = 0.9$	$x_1 = -0.2, x_2 = 1$	$x_1 = -0.2, x_2 = 0.5$
Peak asymmetry	$x_1 = -0.5, x_2 = -0.3$	$x_1 = -0.3, x_2 = 0.4$	$x_1 = -0.3, x_2 = -0.3$	$x_1 = -0.2, x_2 = -0.2$

Experimental design and optimization were performed using Matlab version 8.5.0.197613 (R2015a).

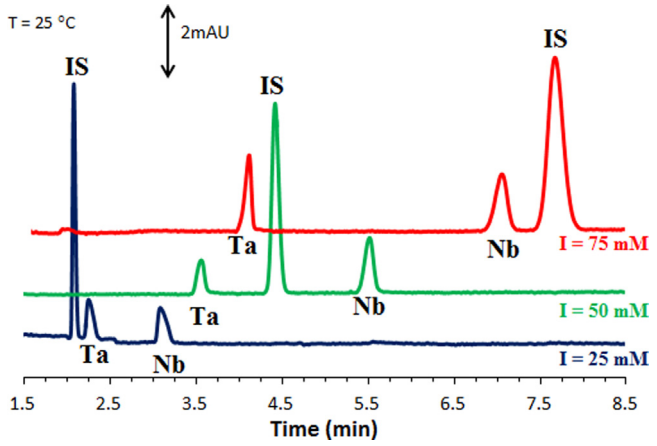

Fig. 2. Electropherograms of solutions containing niobium (Nb), tantalum (Ta) and the internal standard naphatalene-1,5-disulphonate (IS). BGE: 10 mM NaOH + $NaCH_3COO$. I = 25 mM (bottom), 50 mM (middle) or 75 mM (top). T = 25.0 °C. $[Ta_6O_{19}]$ = 0.10 mM. $[Nb_6O_{19}]$ = 0.05 mM. [IS] = 0.17 mM. Other CE conditions: see Fig. 1. Electroosmotic mobility: 63.6×10^{-5} cm^2 s^{-1} V^{-1} (bottom), 53.5×10^{-5} cm^2 s^{-1} V^{-1} (middle) and 48.9×10^{-5} cm^2 s^{-1} V^{-1} (top).

if higher temperatures could have been considered regarding the specifications of the CE system used here, we chose to limit the temperature to 40 °C in order to prevent from premature aging of the bare-fused silica capillary since the analyses were performed in alkaline media. The selected final domains were: $25 \leq I \leq 75$ mM and $25 \leq T \leq 40$ °C. As mentioned above, two independent experimental designs were performed (one with LiOH-$LiCH_3COO$ BGE and one with NaOH-$NaCH_3COO$ BGE) because the nature of the alkaline ion influences the solution chemistry of $H_xNb_6O_{19}{}^{x-8}{}_{(aq)}$ and $H_xTa_6O_{19}{}^{x-8}{}_{(aq)}$ [27–29].

We first expected to find the best separation conditions using a classical response surface methodology, based on optimizing resolution values between peaks while minimizing analysis time. However, as shown in Fig. 2, changes in the migration order of the peaks of hexaniobate, hexatantalate and naphthalene-1,5-disulfonate ions were observed as a function of the ionic strength, at constant temperature with lithium-based electrolytes. Similar observations were made with sodium-based electrolytes.

It is worth noticing that the ionic strength did not change the migration order of Ta and Nb ions, which have very similar electronic and structural features. The migration order observed for $H_xNb_6O_{19}{}^{x-8}{}_{(aq)}$ and $H_xTa_6O_{19}{}^{x-8}{}_{(aq)}$ ions has been explained elsewhere [23]. The variation in the migration order of IS and Nb–Ta with the ionic strength is thought to be due to different effective charges that exhibit $H_xNb_6O_{19}{}^{x-8}{}_{(aq)}$ and $H_xTa_6O_{19}{}^{x-8}{}_{(aq)}$ ($0 \leq x \leq 3$) in Li^+- or Na^+-based BGE compared to naphthalene-1,5-disulfonate, which has only two negative charges at pH 12. Indeed, as observed by Friedl et al. [35], the influence of the ionic strength on electrophoretic mobility of ions is strongly related to the charge of the considered ions. Nevertheless, the use of their empirical equation did not allow a correct fitting of the electrophoretic mobility values that we measured as a function of ionic strength at constant temperature and constant BGE nature. This may be linked to the complexity of the condensation with alkali ions or cation exchange phenomena already observed with the Nb(V) or Ta(V) ions in alkaline media [23,27]. Consequently, an increase in ionic strength reduced the electrophoretic mobilities of our polyanions, which should decrease their migration times with our experimental setting (counter-electroosmotic flow). Nonetheless, an increase in ionic strength also induced a significant decrease (of about 70%) in the electroosmotic flow. This second phenomenon is predominant and explains why the analysis time was drastically lengthened, changing from 3.3 min at I = 25 mM to 8.1 min at I = 75 mM (Fig. 2). Contrary to the ionic strength, the temperature has no effect on the migration order and, as expected, the total analysis time decreases when the temperature increases. However, the migration order of Nb, Ta and IS does not remain constant over the ionic strength domain investigated, as highlighted in Fig. 2.

As a consequence of this change in the migration order, it is obvious that for some conditions, the IS peak overlaps with the Nb or Ta peak. This renders the data treatment more complex because the peak resolutions, which are usually chosen as appropriate responses, are not monotonic functions over the whole experimental domain. For example, it can be inferred from Fig. 2 that the resolution between the peak of Ta and the peak of IS equals zero for one ionic strength value in the domain $25 \text{ mM} \leq I \leq 50$ mM (at T = 25 °C) whereas it is a positive number for the other ionic strength values.

To overcome this issue, new responses were chosen and an ad hoc data treatment was developed as detailed in Section 2.3. The selected responses were start time, migration time and end time for each peak. This type of response was previously used to optimize the CE separation of aromatic hydrocarbons [26]. In our case, the optimization was then focused on finding the conditions where the peaks did not overlap, where the total analysis time was as short as possible, and where the peaks were most symmetric or narrowest, including or not an additional constraint of robustness on the neighboring points of the predicted optimum point. An example of the calculated desirability function for a given set of constraints is detailed in Fig. 3.

3.3. Experimental validation

The 8 predicted optimal points (4 in LiOH–$LiCH_3COO$ BGE and 4 in NaOH–$NaCH_3COO$ BGE) were tested experimentally (Fig. 4). Regarding the four predicted optima in NaOH–$NaCH_3COO$ media, two different domains of I and T values were obtained considering either peak widths or peak symmetries. Nevertheless, the four resulting electropherograms were quite similar. The peaks of Nb, Ta and IS were always baseline resolved and the total analysis times were comprised between 4.1 and 5.5 min. In the case of LiOH–$LiCH_3COO$-based BGEs, the four predicted optimum conditions involved about the same ionic strength value (42.5 or 45 mM) whereas the temperature values varied between −0.3 and 1 in coded values. However, the four resulting electropherograms are also very similar and show that the three peaks were baseline resolved except for one condition (Fig. 4B). Even if the separation was already satisfactory in Na^+-based BGEs, the peak symmetries were slightly better and the total analysis times were all infe-

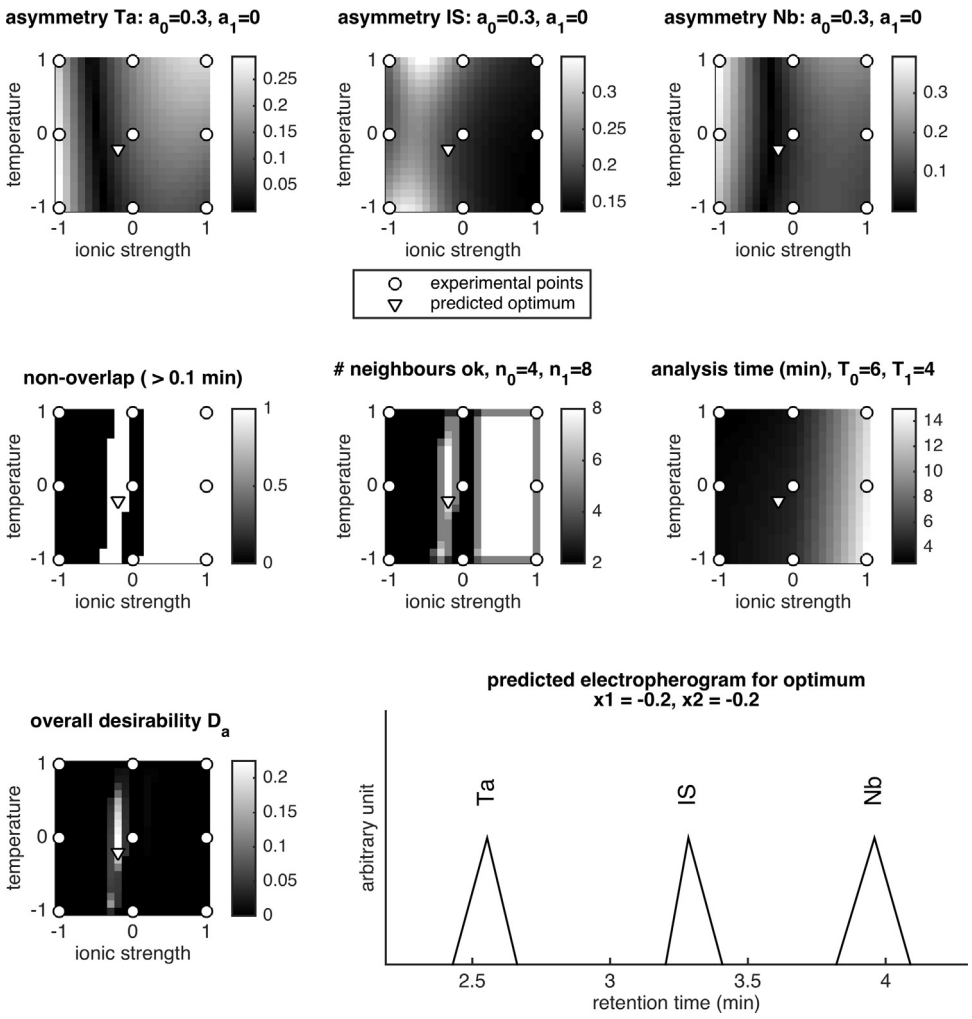

Fig. 3. Detailed analysis of the predicted optimum for counter-ion Li^+, minimizing asymmetry, under the robustness constraint that a maximum number of neighboring pixels do not overlap (grey cell in Table 2). Top graphs: asymmetries $ai(k)$ of each of the 3 components (Ta, IS, Nb). Middle left graph: 1 if minutes (Δtij) > 0.1 min (hard non-overlapping constraint satisfied), else 0. Middle graph: number of neighbors satisfying the hard constraint $n(k)$. Middle right graph: analysis time $T(k)$ in minutes. Bottom middle graph: desirability function D_a. Bottom right graph: predicted (schematic) electropherogram for the predicted optimum (peaks heights are not modeled).

rior to 4.2 min when working with LiOH-$LiCH_3COO$. Taking these results into account, the optimum conditions selected to perform the Nb–Ta separation in the presence of the internal standard (naphthalene-1,5-disulfonate) are a BGE composed of 10 mM LiOH and 35 mM $LiCH_3COO$ (I = 45 mM or −0.2 in coded value) and a temperature of 31.0 °C (-0.2 in coded value), which corresponds to the optimum predicted taking into consideration optimizing the peak symmetries and demanding robustness of predicted neighborhood points. It is also worth noticing that the predicted migration times (Fig. 3) and the experimental ones (Fig. 4B), under the optimal conditions, are in close agreement.

Up to now, all the electropherograms related to the experimental designs were recorded with an applied voltage of 10 kV, which avoids Joule heating even for the samples with the highest ionic strength (checked experimentally). After determining the optimal temperature and ionic strength for the separation, the applied voltage was increased since it is known that it reduces the analysis time without impairing the quality of the separation. Under the optimized conditions, Joule effect tests were performed (measurement of the current intensity versus the applied voltage) in order to evaluate the maximum voltage that could be applied without noticing a detrimental effect due to Joule heating. This led to an increase in the applied voltage from 10 up to 16 kV which induced a decrease in the total analysis time to 2.3 min. The electropherogram of a solution containing Nb, Ta and IS measured under the final optimized conditions is presented in Fig 5. The electropherogram obtained with the previously reported and non-optimized method is also given for comparison. It is clear from the results presented in Fig. 5 that detection sensitivity, peak symmetry, peak width, efficiency and analysis time were greatly improved. The separation with the optimized method was accomplished in 2.3 min which is, to our knowledge, about 3 times faster than any CE method that has ever been reported for the separation of niobium and tantalum.

The robustness of the method with the final conditions (16 kV; I = 45 mM; T = 31.0 °C) was also evaluated (Fig. S2). Electropherograms of a solution containing Nb, Ta and IS were measured when varying the temperature or the ionic strength to ± 1% from their optimal values. The Ta peak was found to be the most sensitive with a standard deviation of 2.5% for its normalized migration time, whereas the corresponding parameter was of 0.7% for Nb. The standard deviations measured for the normalized corrected areas are 2.0% for Ta and 2.1% for Nb. Nonetheless, the total analysis time was lower than 2.5 min and the peaks of Nb, Ta and IS were baseline resolved regardless the tested conditions.

The linearity and quantitation limits of the optimized method were also determined (Fig. S3). The linearity of the method was evaluated by regressing the normalized corrected areas against the total Nb_6O_{19} or Ta_6O_{19} concentrations and using the least-squares

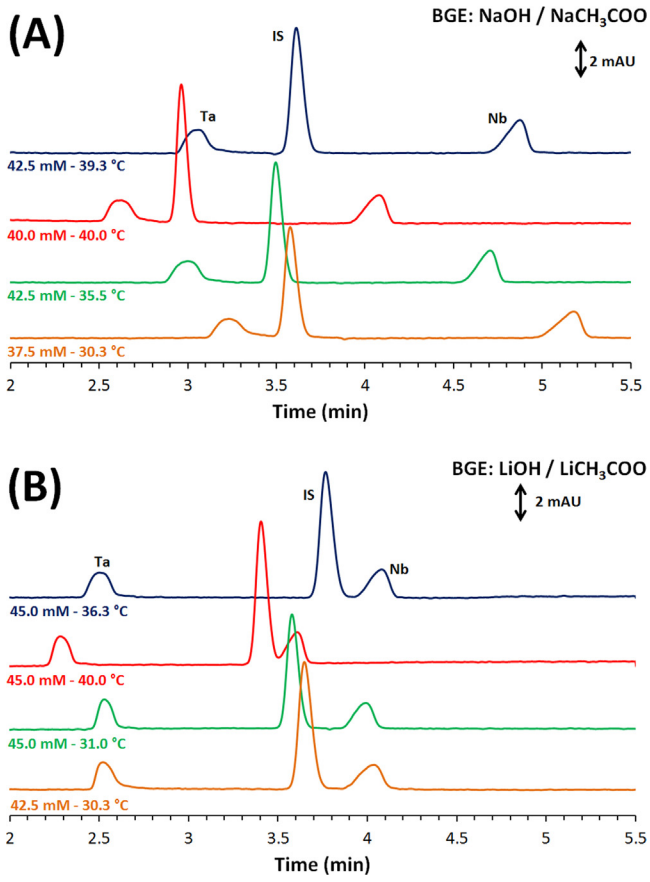

Fig. 4. Electropherograms of solutions containing niobium (Nb), tantalum (Ta) and the internal standard (IS) measured under the predicted optimum conditions. BGE: 10 mM LiOH + $LiCH_3COO$ (A) or 10 mM NaOH + $NaCH_3COO$ (B). $[Ta_6O_{19}]$ = 0.10 mM. $[Nb_6O_{19}]$ = 0.05 mM. [IS] = 0.17 mM. Other CE conditions: see Fig. 1. The ionic strength and the temperature used for the CE separations are indicated below each electropherogram. The corresponding coded values (*I*; *T*) are (from top to bottom): (−0.3; +0.9), (−0.4; +1.0), (−0.3; +0.4), (−0.5; −0.3) in NaOH–$NaCH_3COO$ BGEs and (−0.2; +0.5), (−0.2; +1.0), (−0.2; −0.2), (−0.3; −0.3) in LiOH–$LiCH_3COO$ BGEs. (For interpretation of the references to color in the text, the reader is referred to the web version of this article.)

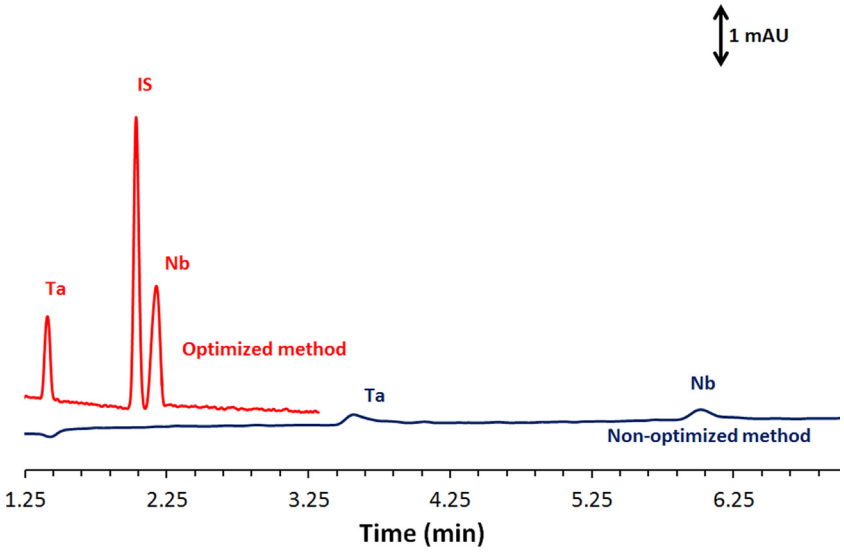

Fig. 5. Top: electropherogram of a solution containing Nb, Ta and IS obtained with the optimized method. BGE: 10 mM LiOH + 35 mM $LiCH_3COO$ (*I* = 45 mM) (BGE similar to Fig. 4B, green line). *U* = 16 kV, *T* = 31.0 °C. $[Ta_6O_{19}]$ and $[Nb_6O_{19}]$ = 0.050 mM. [IS] = 0.085 mM. Bare-fused silica capillary, 50 μm ID × 30 cm (detection at 8.5 cm). λ_{det} = 211 (±5) nm and λ_{ref} = 325 (±50) nm. Electroosmotic mobility = 66.4 × 10^{-5} cm^2 s^{-1} V^{-1}. Bottom: electropherogram of a solution containing Nb and Ta obtained with the initial non-optimized conditions [23]. BGE: 10 mM NaOH + 40 mM NaCl (*I* = 50 mM). *U* = 10 kV, *T* = 25.0 °C. $[Ta_6O_{19}]$ and $[Nb_6O_{19}]$ = 0.125 mM. Bare-fused silica capillary, 50 μm ID × 35 cm (detection at 8.5 cm), λ_{det} = 214 (±2) nm and λ_{ref} = 350 (±40) nm. Electroosmotic mobility = 53.9 × 10^{-5} cm^2 s^{-1} V^{-1}.

Table 3
Linear regression calibration parameters for $H_xNb_6O_{19}^{x-8}$ and $H_xTa_6O_{19}^{x-8}$ ions. Seven concentration levels between 0.02 and 1.00 mM were used for $H_xNb_6O_{19}^{x-8}$ and nine concentration levels between 0.02 and 4.50 mM for $H_xTa_6O_{19}^{x-8}$. CE conditions: see Fig. 5. The calibration curves are given in Fig. S3.

	Ions	
Parameter	Hexatantalate	Hexaniobate
Slope	+8.50	+10.4
Intercept	−0.227	+0.127
σ_y [a]	0.047	0.116
R^2	0.9988	0.9993

[a] Standard error of the *Y* estimates.

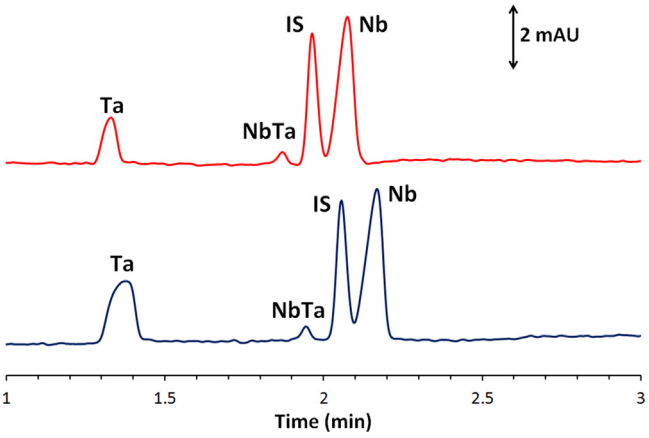

Fig. 6. Electropherogram of an industrial Nb sample spiked with hexatantalate ions. Peak identification: $H_xTa_6O_{19}^{x-8}$ (Ta); $H_xNb_6O_{19}^{x-8}$ (Nb); $H_xNb_5TaO_{19}^{x-8}$ (NbTa); internal standard (IS). Industrial sample diluted 25 times in 10 mM LiOH + 35 mM $LiCH_3COO$ and spiked with 0.09 mM (top) or 0.18 mM (bottom) of $H_xTa_6O_{19}^{x-8}$ ions. T = 31.0 °C. BGE: 10 mM LiOH + 35 mM $LiCH_3COO$ (I = 45 mM). U = 16 kV.

method (Table 3). The method was linear up to 4.5 mM for hexatantalate ions, and up to 1.0 mM for hexaniobate ions. The upper limit for Nb is governed by peak overlapping between Nb and IS. The limits of quantitation, calculated considering a signal to noise ratio of 10, were estimated at 0.016 mM for $H_xNb_6O_{19}^{x-8}$ and 0.022 mM for $H_xTa_6O_{19}^{x-8}$. These values led to a quantitation domain of 9 to 557 mg L^{-1} for Nb and 24 to 4,890 mg L^{-1} for Ta. By comparison, the Nb and Ta concentrations encountered in industrial processes are typically higher than 100 mg L^{-1} [15,36,37].

3.4. Application to a real sample

The optimized method was then applied to the determination of Nb and Ta in a real alkaline industrial sample provided by Eramet Research company (France). This sample differs slightly from the model samples we used because it was composed of pure hexaniobate ions ($[Nb_6O_{19}]$ = 3.40 ±0.17 mM) and also mixed Nb–Ta polyoxometalates ($[Nb_5TaO_{19}]$ = 0.227 ±0.011 mM). The insertion of Ta into hexaniobate ions is inherent to the process used by the company. Taking into account that Nb and Ta have very similar chemical properties, the separation of the pure ions $H_xNb_6O_{19}^{x-8}$ and the substituted ions $H_xNb_6Ta_6O_{19}^{x-8}$ seemed challenging. Nonetheless, we applied our optimized CE method to the industrial sample and we also spiked it with pure hexatantalate ions in order to evaluate the potential separation of $H_xNb_6O_{19}^{x-8}$, $H_xTa_6O_{19}^{x-8}$ and $H_xNb_5TaO_{19}^{x-8}$ ions (Fig. 6).

As shown in Fig. 6, the separation between $H_xNb_6O_{19}^{x-8}$, $H_xTa_6O_{19}^{x-8}$ and $H_xNb_5TaO_{19}^{x-8}$ ions is accomplished in less than 2.3 min with our optimized method. The small peak at 1.9 min was attributed to the substituted ions $H_xNb_5TaO_{19}^{x-8}$ taking into account the migration times, the expected concentrations and the UV absorbance spectra of the different peaks. It should be noted that the separation of the three polyoxoanions $H_xNb_6O_{19}^{x-8}$, $H_xTa_6O_{19}^{x-8}$ and $H_xNb_5TaO_{19}^{x-8}$ indicates that they are not in a dynamic fast kinetic equilibrium since only kinetically inert species can be separated by conventional CE [38]. The IS peak and the Nb peak slightly overlap, but with a resolution value of 1.4 which allows correct quantitation, and the Ta peak is slightly broader than for the standard solutions. This is thought to be due to the presence of interfering ions in the industrial sample (54 mM of Na^+ ions, etc) that may induce some destacking. The $H_xNb_6O_{19}^{x-8}$ concentration determined by the CE method is 3.53 ±0.07 mM (5 repetitions), which is in the range given by the industrial (3.40 ±0.17 mM), thereby demonstrating the applicability of CE to perform the determination of Nb and Ta in real alkaline solutions.

4. Conclusion

For the first time, a CE method was developed for the analysis of Nb and Ta in alkaline media. The separation is performed with classical bared-fused silica capillary and does not require any chelating or chromophoric reagent. First, based on a method designed for speciation studies, we optimized the detection conditions and the nature of the BGE co-ion, and we found a suitable internal standard for the analysis of $H_xNb_6O_{19}^{x-8}$ and $H_xTa_6O_{19}^{x-8}$ ions. Two experimental designs were then performed in order to find the best ionic strength and temperature for the separation, in both Li- and Na-based BGEs. Unfortunately, the ionic strength influences the migration order between IS and Nb–Ta, which necessitated an optimized data treatment. The original data processing used allowed predicting 8 optimal conditions which were then tested experimentally. The final separation conditions involved a BGE composed of 10 mM LiOH + 35 mM $LiCH_3COO$ (I = 45 mM) and a temperature of 31.0 °C. The applied voltage was next optimized and the separation of $H_xNb_6O_{19}^{x-8}$, $H_xTa_6O_{19}^{x-8}$ and IS was performed in 2.3 min, which is three times faster than any CE method reported so far for the separation of Nb and Ta (acidic media included). Some figures of merit of the methods were also determined. The quantitation limits (S/N = 10) are 0.016 mM for $H_xNb_6O_{19}^{x-8}$ and 0.022 mM for $H_xTa_6O_{19}^{x-8}$ and the linearity is extended to 1.0 mM for $H_xNb_6O_{19}^{x-8}$ and 4.5 mM for $H_xTa_6O_{19}^{x-8}$. Finally, the optimized method was successfully applied to a real Nb–Ta industrial sample. Furthermore, the separation was pushed to the separation of the non-substituted ions ($H_xNb_6O_{19}^{x-8}$, $H_xTa_6O_{19}^{x-8}$) and the substituted ones ($H_xNb_5TaO_{19}^{x-8}$). Our optimized method will be used in a future work to probe the formation of other substituted niobium-metal polyoxometalates. An ongoing work is also focused on the development of a semi-quantitative method, without internal standard, for the ultra-fast screening of hexaniobate and hexatantalate ions.

Acknowledgment

Financial support from ERAMET Research (France) is gratefully acknowledged.

Appendix A. Supplementary data

Supplementary data associated with this article can be found, in the online version, at http://dx.doi.org/10.1016/j.chroma.2016.01.075.

References

[1] Roskill Information Services, The Economics of Niobium, Roskill Information Services, London, 2009.

[2] E.E. Nikishina, D.V. Drobot, E.N. Lebedeva, Niobium and tantalum state of the world market, apllication fields, and sources of raw materials. Part 1, Russ. J. Non-Ferr. Met. 54 (2013) 446–452.
[3] U.S. Geological Survey, K. Schulz, J. Papp, Niobium and Tantalum-Indispensable Twins http://pubs.usgs.gov/fs/2014/3054/pdf/fs2014-3054.pdf, 2015 (accessed 18.09.15).
[4] ITER Organization, ITER Mag N°5, Www.iter.org. https://www.iter.org/fr/mag/5/40, 2015 (accessed 25.06.15).
[5] S.R. Taylor, Abundance of chemical elements in the continental crust: a new table, Geochim. Cosmochim. Acta 28 (1964) 1273–1285.
[6] BRGM, Panorama 2010 du marché du niobium, http://infoterre.brgm.fr/rapports/RP-60579-FR.pdf, 2011.
[7] European Commission, Report on Critical Raw Materials for The EU, 2014.
[8] R. Shannon, Revised effective ionic radii and systematic studies of interatomic distances in halides and chalcogenides, Acta Crystallogr. A 32 (1976) 751–767.
[9] H. Matsumiya, S. Yasuno, N. Iki, S. Miyano, Sulfinylcalix[4] arene-impregnated Amberlite XAD-7 resin for the separation of niobium(V) from tantalum(V), J. Chromatogr. A 1090 (2005) 197–200, http://dx.doi.org/10.1016/j.chroma.2005.06.086.
[10] L. Dongling, H. Xiaoyan, W. Haizhou, Separation and simultaneous determination of niobium and tantalum in steel by reversed-phase high-performance liquid chromatography using 2-(2-pyridylazo)-5-diethylamino phenol as a pre-column derivatizing reagent, Talanta 63 (2004) 233–237, http://dx.doi.org/10.1016/j.talanta.2003.09.028.
[11] A. Agulyanski, The Chemistry of Tantalum and Niobium Fluoride Compounds, 1st ed., Elsevier, Amsterdam, Boston, 2004.
[12] Z. Zhu, C.Y. Cheng, Solvent extraction technology for the separation and purification of niobium and tantalum: a review, Hydrometallurgy 107 (2011) 1–12, http://dx.doi.org/10.1016/j.hydromet.2010.12.015.
[13] H. Zhou, S. Zheng, Y. Zhang, D. Yi, A kinetic study of the leaching of a low-grade niobium–tantalum ore by concentrated KOH solution, Hydrometallurgy 80 (2005) 170–178, http://dx.doi.org/10.1016/j.hydromet.2005.06.011.
[14] X. Wang, S. Zheng, H. Xu, Y. Zhang, Leaching of niobium and tantalum from a low-grade ore using a KOH roast–water leach system, Hydrometallurgy 98 (2009) 219–223, http://dx.doi.org/10.1016/j.hydromet.2009.05.002.
[15] Eramet, F. Delvalle, F. Lachaize, V. Weigel, Method for Purifying Niobium and/or Tantalum, Patent: WO 2015/004375 A1, 2015.
[16] G.J.-P. Deblonde, A. Moncomble, G. Cote, S. Bélair, A. Chagnes, Experimental and computational exploration of the UV–visible properties of hexaniobate and hexatantalate ions, RSC Adv. (2015) 7619–7627, http://dx.doi.org/10.1039/C4RA14866E.
[17] A.R. Timerbaev, O.P. Semenova, P. Jandik, G.K. Bonn, Metal ion capillary electrophoresis with direct UV detection. Effect of a charged surfactant on the migration behaviour of metal chelates, J. Chromatogr. A 671 (1994) 419–427.
[18] B.-F. Liu, L.-B. Liu, H. Chen, J.-K. Cheng, Separation of vanadium, niobium and tantalum as ternary mixed-ligand complexes by capillary electrophoresis using chelation with 4-(2-pyridylazo) resorcinol and tartaric acid, Fresenius J. Anal. Chem. 369 (2001) 195–197.
[19] E.-B. Liu, Y.-M. Liu, J.-K. Cheng, Separation of niobium(V) and tantalum(V) by capillary electrophoresis with chemiluminescence detection, Anal. Chim. Acta 443 (2001) 101–105.
[20] N. Vachirapatama, P. Doble, Z. Yu, M. Macka, P.R. Haddad, Separation of niobium (V) and tantalum (V) as ternary complexes with citrate and metallochromic ligands by capillary electrophoresis, Anal. Chim. Acta 434 (2001) 301–307.
[21] B. Sun, M. Macka, P.R. Haddad, Trace determination of arsenic species by capillary electrophoresis with direct UV detection using sensitivity enhancement by counter- or co-electroosmotic flow stacking and a high-sensitivity cell, Electrophoresis 24 (2003) 2045–2053, http://dx.doi.org/10.1002/elps.200305447.
[22] B. Sun, M. Macka, P.R. Haddad, Speciation of arsenic and selenium by capillary electrophoresis, J. Chromatogr. A 1039 (2004) 201–208, http://dx.doi.org/10.1016/j.chroma.2004.03.045.
[23] G.J.-P. Deblonde, N. Delaunay, D. Lee, A. Chagnes, G. Cote, First investigation of polyoxoniobate and polyoxotantalate aqueous speciation by capillary zone electrophoresis, RSC Adv. 5 (2015) 64119-–64124, http://dx.doi.org/10.1039/C5RA11521C.
[24] M. Nyman, Polyoxoniobate chemistry in the 21st century, Dalton Trans. 40 (2011) 8049, http://dx.doi.org/10.1039/c1dt10435g.
[25] L. Ferey, N. Delaunay, D.N. Rutledge, A. Huertas, Y. Raoul, P. Gareil, et al., Use of response surface methodology to optimize the simultaneous separation of eight polycyclic aromatic hydrocarbons by capillary zone electrophoresis with laser-induced fluorescence detection, J. Chromatogr. A 1302 (2013) 181–190, http://dx.doi.org/10.1016/j.chroma.2013.06.027.
[26] L. Ferey, N. Delaunay, D.N. Rutledge, A. Huertas, Y. Raoul, P. Gareil, et al., An experimental design based strategy to optimize a capillary electrophoresis method for the separation of 19 polycyclic aromatic hydrocarbons, Anal. Chim. Acta 820 (2014) 195-–204, http://dx.doi.org/10.1016/j.aca.2014.02.040.
[27] G.J.-P. Deblonde, A. Chagnes, S. Bélair, G. Cote, Solubility of niobium(V) and tantalum(V) under mild alkaline conditions, Hydrometallurgy 156 (2015) 99–106, http://dx.doi.org/10.1016/j.hydromet.2015.05.015.
[28] M.R. Antonio, M. Nyman, T.M. Anderson, Direct observation of contact ion-pair formation in aqueous solution, Angew. Chem. Int. Ed. 48 (2009) 6136–6140, http://dx.doi.org/10.1002/anie.200805323.
[29] L.B. Fullmer, P.I. Molina, M.R. Antonio, M. Nyman, Contrasting ion-association behaviour of Ta and Nb polyoxometalates, Dalton Trans. 43 (2014) 15295–15299, http://dx.doi.org/10.1039/C4DT02394C.
[30] N.R. Draper, H. Smith, Applied Regression Analysis, 3rd ed., Wiley, 1998.
[31] D.L. Massart, B.G.M. Vandeginste, L.M.C. Buydens, S. De Jong, P.J. Lewi, J. Smeyers-Verbeke, Handbook of Chemometrics and Qualimetrics: Part A, Elsevier, Amsterdam, 1997.
[32] G. Derringer, R. Suich, Simultaneous optimization of several response variables, J. Qual. Technol. 12 (1980).
[33] P. Bocek, M. Deml, P. Gebauer, V. Dolnik, in: Herausgegeben von, B.J. Radola (Eds.), Analytical Isotachophoresis, VCH Verlagsgesellschaft Weinheim, Basel, Cambridge, New York, 1988.
[34] A.K. SenGupta, Y. Marcus, J.A. Marinsky, Ion Exchange and Solvent Extraction, Marcel & Dekker Inc., NewYork, Basel, 2005.
[35] W. Friedl, J.C. Reijenga, E. Kenndler, Ionic strength and charge number correction for mobilities of multivalent organic anions in capillary electrophoresis, J. Chromatogr. A 709 (1995) 163–170, http://dx.doi.org/10.1016/0021-9673(95) 00159-K.
[36] F. Fairbrother, The Chemistry of Niobium and Tantalum, Elsevier, Amsterdam, London, New York, 1967.
[37] V.G. Maiorov, A.I. Nikolaev, V.K. Kopkov, V.Y. Kuznetsov, N.L. Mikhailova, Preparation of alkaline solutions of niobium(V), Russ. J. Appl. Chem. 84 (2011) 1137–1140, http://dx.doi.org/10.1134/S1070427211070020.
[38] M. Macka, P.R. Haddad, Determination of metal ions by capillary electrophoresis, Electrophoresis 18 (1997) 2482–2501.